

Automatic Sea Floor Characterization based on Underwater Acoustic Image Processing

CRISTIAN MOLDER, MIRCEA BOȘCOIANU, MIHAI I. STANCIU, IULIAN C. VIZITIU

Military Technical Academy

Department of Electronics and Informatics

George Coșbuc street 81-83, Bucharest

ROMANIA

cristianmolder@gmail.com <http://www.mta.ro>

Abstract: Automatic sea floor characterization is mainly based on the signal or image processing of the data acquired using an active acoustic system called sediment sonar. Each processing method suits a specific type of sonar, such as the monobeam, the multibeam, or the side-scan sonar. Most types of sonar offer a two dimensional view of the sea floor surface. Therefore, a high resolution image results which can be further analyzed. The inconvenient is that the sonar cannot view inside of the sea floor for a deeper analysis. Therefore, lower frequency acoustic systems are used for in-depth sea floor penetration (boomer, sparker, airguns or sub-bottom profilers). In this case, a mono dimensional signal results. Previous studies on the low-frequency systems are mainly based on the visual inspection by a geological human expert. To automatize this process, we propose the use of feature sets based on the transposed expert fuzzy reasoning. Two features are extracted, the first based on the sea floor contour and the second based on the sub-bottom sediment texture.

Key-Words: Sedimentology, Underwater Acoustics, Pattern Recognition, Image Processing, Textures, Wavelets

1 Introduction

Sea floor acoustics are based on the emission of a modulated or a bandwidth low-frequency signal (usually in the 0.5 - 100 kHz band) followed by the analysis of the received signal from the sea floor. The response is influenced by the interaction between the acoustic wave and the sedimentary structure. Some authors tried to model these interactions depending on the particle size and spatial arrangement, the layer pressure, or the saturation percentage [29, 10, 15]. Unfortunately, these models cannot include all the interactions that occur in the geological structure complexity [14, 6].

Nowadays, most of the monodimensional low-frequency sub-bottom seismic recordings using a specialized sonar are interpreted by a human geological expert by reading from a display or a printed paper [27]. Therefore, an automatic algorithm was created with the purpose to eliminate the human expertise by transposing his fuzzy reasoning into new features.

Following discussions with geological experts, the two main visual characteristics observed by a data analyzer are the geometric shape of the sea bottom (horizons) and the sub-bottom aspect of the sediment structures. Using this information, two feature sets can be obtained. The next section presents the visual characteristics of the main sediment classes based on

human expert fuzzy reasoning. The two proposed feature sets are explained in the second part of the paper. The last section contains experimental results, conclusion and further work.

2 Human expert fuzzy reasoning

In the sea, uncountable sedimentary level configurations can be observed. The acoustic response is based on the interaction between the incident wave and the sediment geological characteristics (particle shapes and sizes, layer structure). The response is also clearer when the difference of impedance between two layers is bigger.

For sedimentary layers with homogeneous structure and composition, the acoustic response is also homogeneous and uniform along the whole layer. Because of physical and chemical interactions with the sea (tides, waves, streams, sea plants and animals), as well as the human intervention, those structures can be modified [4]. For example, agglomeration caused by tides or waves leads to parallel superficial layers with strong contrast (Fig. 1).

Sediment layers composed of various size particles deposit larger particles towards the bottom, while smaller particles remain at the layer surface or in suspension. If the stream have a certain orientation, spe-

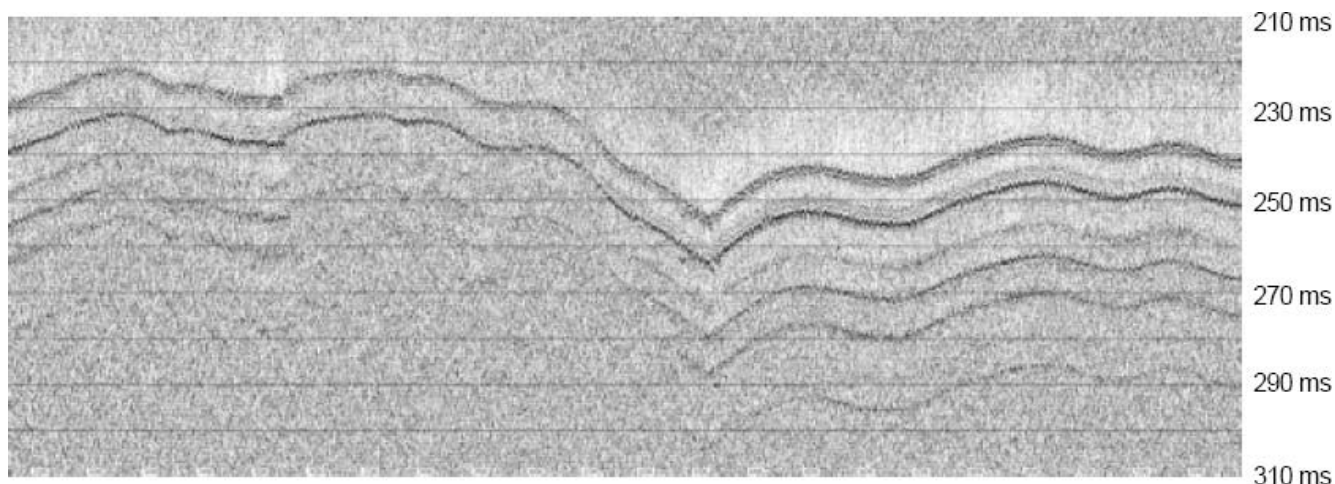


Figure 1: Sedimentary structure on multiple layers (sand)



Figure 2: Surface agglomeration (sand) on a hard layer (rock)

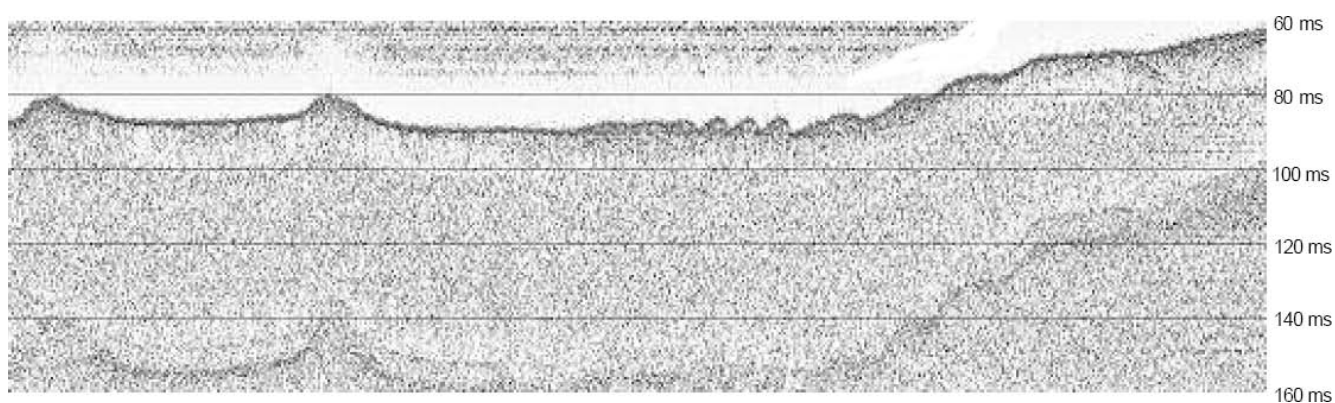


Figure 3: Sand dunes and sand depots on rock layer

cific *sand dunes* shapes can occur (Fig. 3).

The particle size can also determine the sediment layer shape. Most of the time, the *rocks* form a rigid and consolidated structure. This type of structure is not influenced by natural factors such as tides or

streams. The erosion is small because of the superficial layers (*sand* or *mud*) which lay on the rock structure. The shape can be in the same time smooth and rough on portions. When the stream is low, the superficial sediments will consolidate into heavier struc-

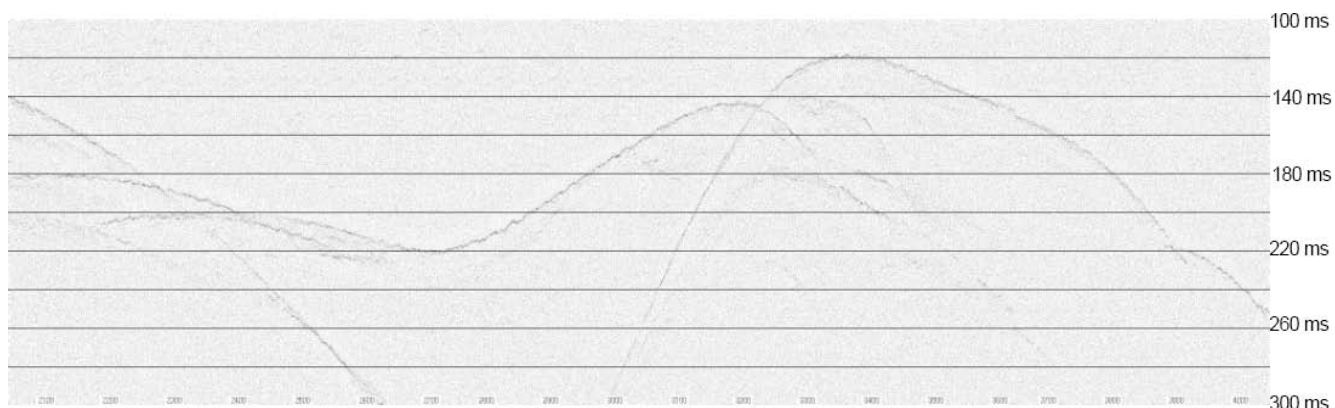


Figure 4: Hyperbolic structures for deeper sea floors (rock)

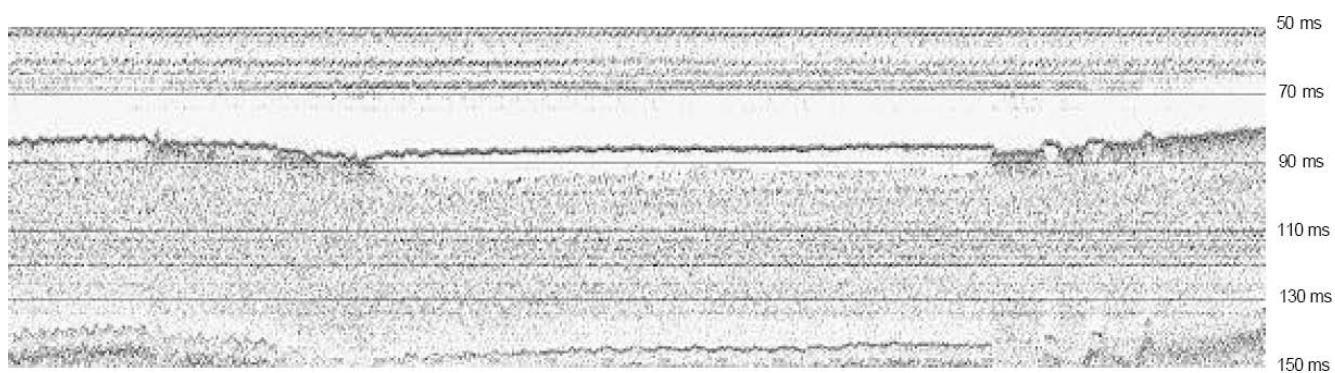


Figure 5: Mud depot on hard layer (rock)

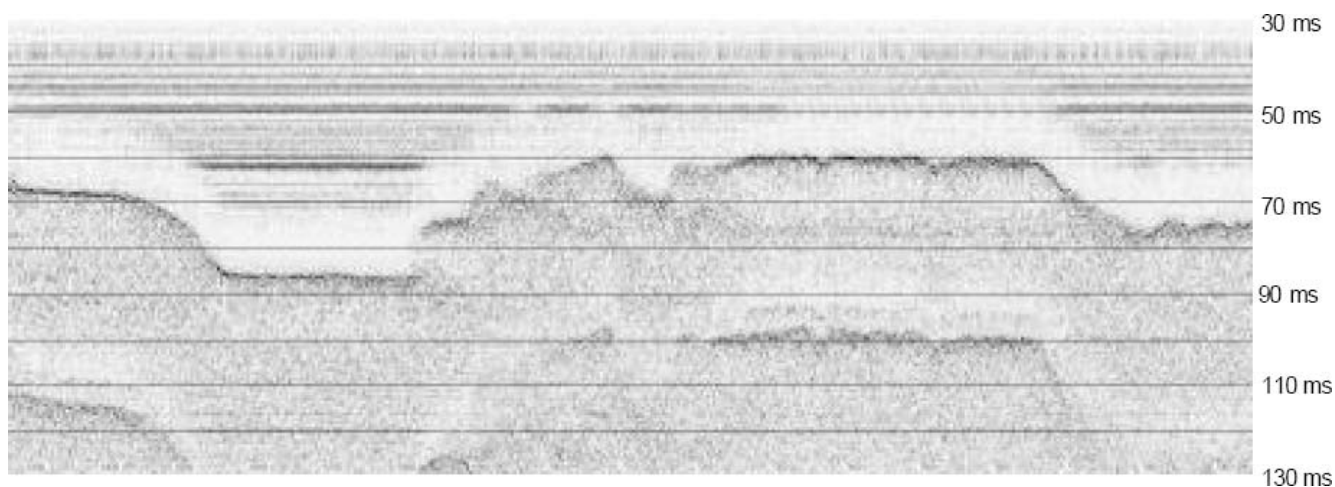


Figure 6: Fine surface depots on a rough hard structure

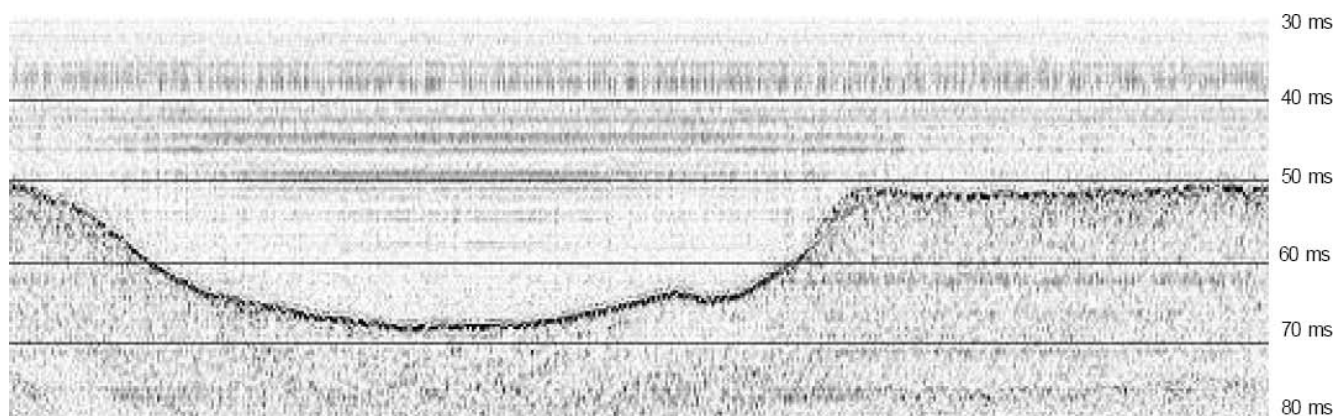


Figure 7: Hard layer (rock) at the sea bottom surface

tures who keep the initial shape (Fig. 2). When rocks reach the sea bottom surface, the horizon shape becomes abrupt. In this case the acoustic response is unclear because of the surface irregularities. The signal cannot penetrate, hence there is no further acoustic response from the inside of the structure. Another type of response is hyperbolic, caused by lateral echoes of the hard structures. This response is typical for deeper sea floors (Fig. 4).

Some fine sediments (e.g., the *mud* or *fine sand*) are completely penetrable by the acoustic signal, which leads to a clear, non-reflexive response. The only response is caused by the impedance difference between the water and the sediment. Most of the fine sediment layers are found at the surface of the sea bottom. Therefore, the second layer is always clearly visible (Fig. 5).

Other sediments, like the *peat*, are not penetrative for the acoustic signal. Therefore, the second layer is never visible. This kind of response is specific for sedimentary layers resulted from rich biological activities (organic decompositions). A *gas* source is obtained in the deeper layers, from volcanic activities inside the tectonic structure. The resulted responses are known as "popmarks". Their structure is easy recognizable, as it grows from inside until the surface of the sea bottom, creating small craters.

Sand depots can be found under many shapes because of their great dynamic and mobility. When the stream is low, the horizons are clear and smooth. The acoustic response is proportional with the particles size and depot structure. The rougher the sand is, the weaker the acoustic response gets. When the stream is high enough, the layer has a specific shape which follows the stream direction.

Salt can also be found in sedimentary structures. The specific shape has a dune aspect which rises until the sea bottom surface, with a hyperbolic structure. The sand layers absorb the acoustic signal. Hence,

the response has small intensity.

The horizon shape determine the shape of all layers. The most frequent situation is being found for rocks. A concave rocky structure favor the sediments with great dynamic (sand, mud). Also, the rocky structures which form small mountains are causing lateral sediment depots (Fig. 6). In this late configuration, rock and sand can be often confused (Fig. 7).

Based on the previous observations made by human experts, one can create two fuzzy features that will serve in an automatic sediment characterization system. The first feature characterize the horizon shape and it is extracted as a contour. The second feature is specific for the acoustic response of the sediment below the horizon and it is extracted as a texture.

For every important type of sediment there is an associated configuration of the two fuzzy features, presented in Table 1. Using these information, quantitative features must be extracted from the acoustic response.

3 Acoustic image analysis

To analyze an acoustic response, pseudo-images are formed from mono-dimensional echoes. As the sonar is running at a constant speed and in a straight direction, the echoes are concatenated to form a matrix which is further used as an acoustic image.

From the resulting acoustic image, two main attributes are considered. The first is represented by the shape of the sea-bottom (the horizon) and the second is based on the textural information which is situated under the horizon (Fig. 9).

3.1 Sediment contour features

Using the shape of the sea bottom horizon, contour-based features can be extracted. Therefore, the extrac-

Table 1: Sediment characterization using textural (acoustic response) and geometrical (horizon) fuzzy features

Sediment type	Acoustic response	Horizon geometry
Mud	Very clear, permeable	Mostly horizontal, smooth
Fine sand	Clear, permeable	Mostly horizontal, smooth
Sand	Slightly clear	Mostly horizontal, smooth
Rock	Slightly clear, impermeable	All configurations, rough
Grit	Slightly clear	Mostly horizontal, smooth
Salt	Slightly clear, few reflections	Hyperbolic, isolated (dunes)
Gas	Opaque, no reflections	Isolated structures
Peat	Opaque, no reflections	Mostly horizontal, smooth

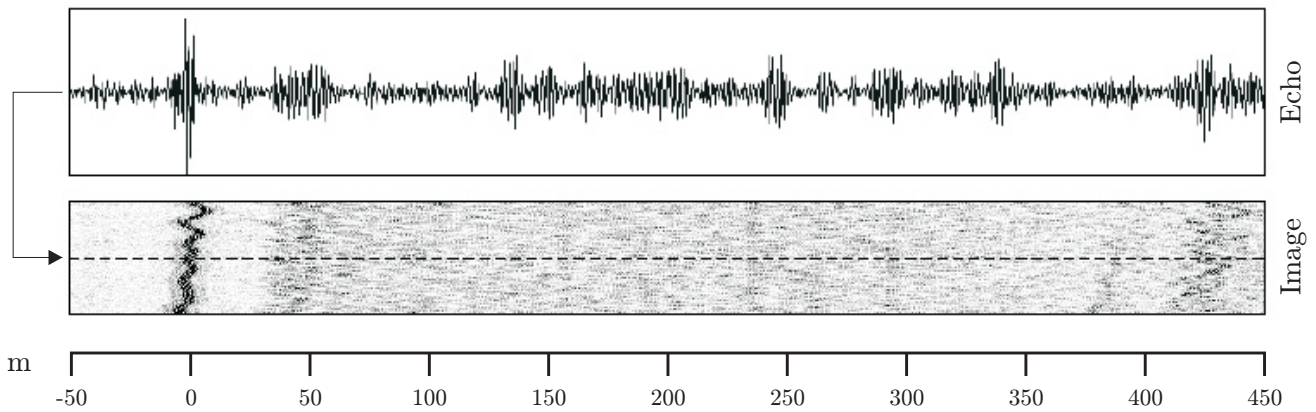


Figure 8: Construction of an acoustic image from echoes. The mono-dimensional responses from the sonar are concatenated into a matrix which forms the acoustic image (90 degrees rotation left)

tion of the contour from the acoustic images is needed first. The free-form active contours [5, 7, 13] are used to obtain an analytic description of the horizons. The possible use of the contour parameters represents an advantage.

The free-form active contour is described using piecewise cubic polynomial segments $y_i(x)$ (Fig. 10). The cubic form offers the possibility of obtaining complex shapes with a minimum ripple comparing to higher degree polynomials [9].

$$y_i(x) = a_i x^3 + b_i x^2 + c_i x + d_i, \quad (1)$$

where i is the segment index, and x takes values in the interval $[0, 1]$.

The active contour convergence is obtained by minimizing an objective function $f(s)$ which takes into account the curve variation limits and the acoustic image intensity.

$$f(s) = w_i f_i(s) + w_c f_c(s), \quad (2)$$

where $f(s)$ is the global objective function, $f_i(s)$ is the image-based local objective function, $f_c(s)$ is the contour-based local objective function, and w_i and w_c are the weights associated to the local objective functions, respectively. By varying the two weights, we

can control the importance of each of the local objective functions.

The image-based objective function $f_i(s)$ attracts the active contour towards the image regions which contain useful information. In our case, the information is represented by the acoustic response high values corresponding to the first horizon (the sea bottom). To ensure a faster convergence, a median filtered version of the acoustic image is preferred (Fig. 11).

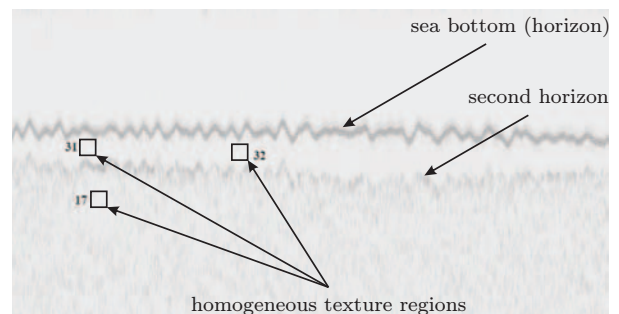


Figure 9: Acoustic image regions of interest. Horizons and homogeneous texture regions are considered for feature extraction

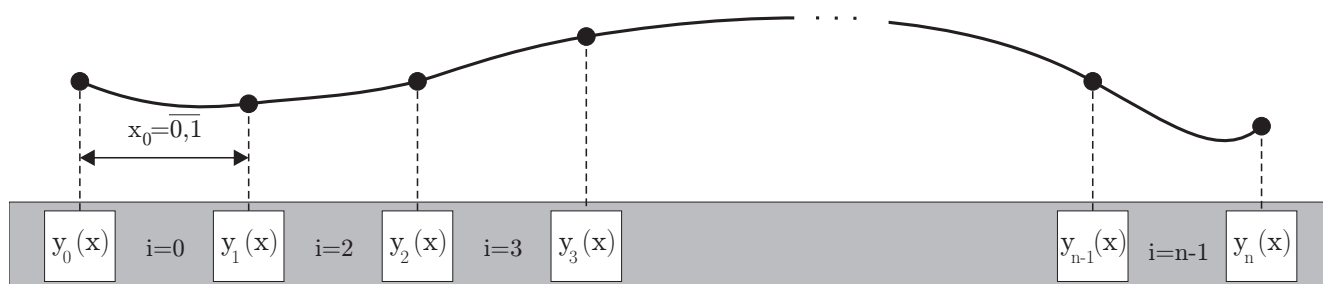


Figure 10: Free-form active contour. The contour is described using piecewise cubic Hermite polynomials

The acoustic image can be divided into constant width vertical slices. For each slice, a piecewise polynomial is considered. When two adjacent polynomials join, the local geometrical parameters must be equal. Moreover, as the sea floor can be considered as a holomorphic function, the piecewise polynomial geometrical parameters cannot exceed certain limits. Therefore, the terminal tangent angles θ take values in the ± 90 degrees interval.

Before convergence, the solution is initialized using a local maxima criterion. Every piecewise polynomial segment is based on maxima detected in its corresponding acoustic image slice. Therefore, for each point of the contour, the optimization will consider a limited vertical variation of k pixels.

The two parameter limits (for tangent angle θ and point variation k) are included in the contour-based objective function $f_c(s)$.

To ease the contour control during optimization, the use of Hermite piecewise polynomials is preferred. A Hermite curve is defined using four parameters: the begin and the end vertices and their corresponding tangents. In the optimization process, the importance of the local objective functions is considered equal. Hence, w_i and w_c are identical.

The optimization method is based on genetic algorithms (GA) because of its simplicity and rapid convergence due to the near-solution initialization. Therefore, the number of iterations required is small (the solution is obtained after 150 iterations). The GA parameters are: population of 100 offsprings, probability of mutation of 0.1, and probability of crossover of 0.5. For images of 1000×700 pixels and for slices of 11 pixels width, chromosomes with 90 genes have been constructed.

The resulting optimized contours are revealing the small details of the sedimentary structures, considering the resolution of the acoustic image. The horizontal distance between two consecutive pixels is 1 m, considering a constant sonar speed of 5 m/s, a signal emission period of 200 ms, a 3.5 kHz chirp signal, and a 12 kHz sampling frequency [2].

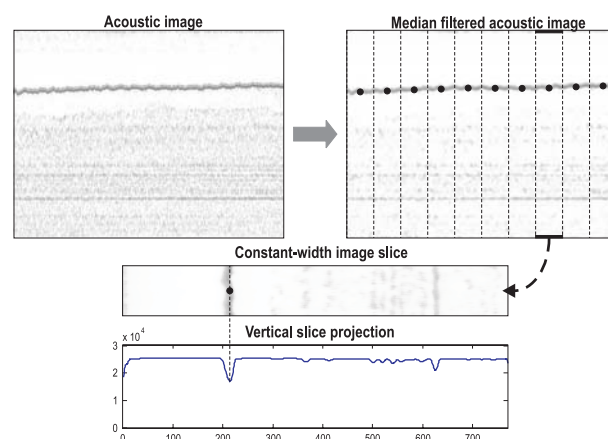


Figure 11: Objective function initialization. The acoustic image is first filtered for faster convergence and each slice contains a maxima-based initial vertex solution

The extracted contours, such as those in Fig. 12, can be further used in a classification system.

The features used as inputs can be the contour parameters or other derived properties such as the local curvature or roughness [30, 1, 17].

3.2 Sediment textural features

Textures can be classified in two main groups: structural and statistical [12, 25]. We use two features extracted with two different methods: the co-occurrence matrices and the Wavelet transforms. The choice is justified by the simultaneous statistical and spectral texture characterization.

The features extracted from the co-occurrence matrices characterize statistical texture properties, hence exploiting the size and orientation of the structural micro-elements.

The Wavelet 2D transforms decompose and analyze the information in the spectral domain. Hence, they offer a multi-resolution approach. This is justified by the fact that the human brain perception of an image is made by analyzing it at different lev-

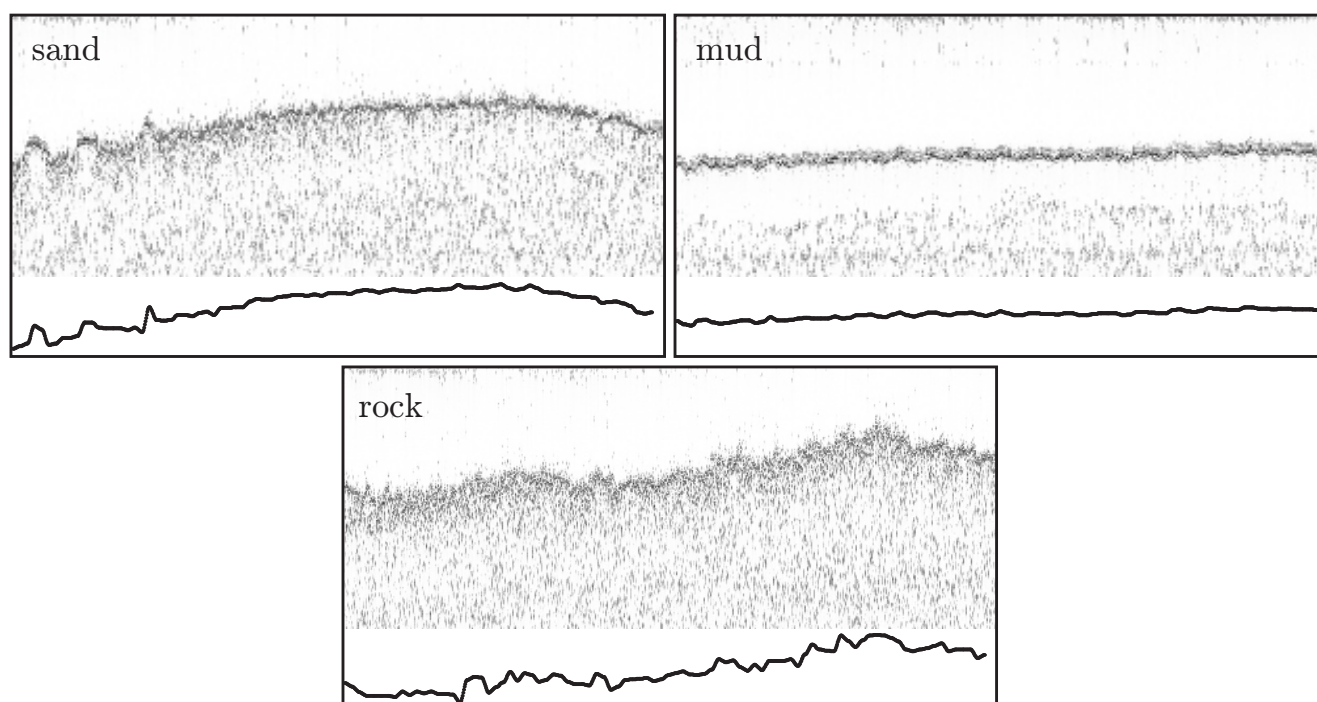


Figure 12: Contour extraction results for different types of horizons: slightly smooth (top left), smooth and horizontal (top right), and rough (bottom)

els of resolution and frequencies. Several Wavelet transforms have been used, such as the Wavelet 2D, Wavelet Packet 2D and the Over-Sampled Wavelet 2D transforms [26]. The later offers translation invariant descriptors and information redundancy.

The two methods are complementary and easy to implement on dedicated hardware.

The *co-occurrence matrix features* are used in the estimation of texture statistics [11]. The textures used for analysis are usually squared. In this article we propose the use of irregular texture shapes. This is justified by the fact that the distance between the sediment layers is very small. Hence, a rectangular texture with sufficient information cannot be extracted. Therefore, we prefer to use irregular shaped regions, cropped between the layers.

The seven co-occurrence features used are the homogeneity, the contrast, the entropy, the correlation, the directivity, the uniformity, and the maximum probability [11, 3]. The co-occurrence matrices are computed for 0, 45, 90 and 135 degrees. For each texture 28 features results. Therefore, a linear dimensionality reduction is applied using the Principal Component Analysis (PCA) [8, 28]. From the latency matrix associated to the eigenvalues, we retain the two first components for further consideration (Fig. 13).

Three *wavelet features* must be extracted from the transforms coefficients due to their great dimensionality. The features are the energy, the entropy, and the

mean value [26]. Those features are computed for every level of the spectral decomposition. A number of 4 decomposition levels was used.

The choice for the mother wavelet is not critical [16, 22, 20, 21]. Several functions are used (Haar, Daubechies 3, Biorthogonal 3.3, Symlet 4, and Coiflet 1) for a potentially classification influence. The classic Wavelet 2D decomposition (W2D) gives a number of $N = L \times 4$ subimages, while the Wavelet Packet 2D (WP2D) and the Over-Sampled Wavelet 2D decompositions (OSW2D) give $N = \sum_{l=1}^L 2^{2n}$. Therefore, a new linear dimensionality reduction must be performed. Using the PCA, we observed that the number of principal components required for the Wavelet Packet 2D was large enough to discard the further use of this transform. Hence, we will consider only the use of the two remaining transforms [23, 24, 18, 19].

As the dimensionality reduction leads to more than 3 components, a visual inspection for the clustering results is not possible. Therefore, a MLP classifier was used. The classification results are very encouraging, and confirm the expectations (Table 2).

4 Conclusions and further work

The main target of this study was to demonstrate the possibility of transposing the human expert fuzzy rea-

Table 2: MLP classification testing results based on wavelet textural features

Transform	Topology	Haar	Db 3	Biorth 3.3	Symlet 4	Coiflet 1
W2D	12:15:1	97.4%	97.7%	98.2%	97.8%	97.7%
OSW2D	5:15:1	95.2%	98.9%	98.4%	98.6%	98.0%

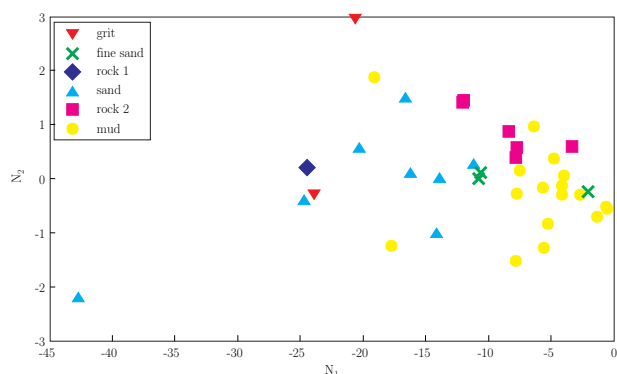


Figure 13: Principal component clustering projection for textural co-occurrence features. The best clusters are obtained for mud, sand and rock

soning into quantifiable measures. The two main subjective observations made by such an expert are the visual characterization of the sea bottom using the horizon contour-like shape and the texture structure under the corresponding horizon. Based on those remarks, two feature sets are proposed. The first is represented by the use of a parametric contour that best describes the sea bottom horizons, and the second is the use of textural features extracted from the acoustic image region below the horizon.

The active contour represents a good method for the extraction of a sub-bottom horizon. The layer can be described as a holomorphic function. Hence, a cubic piecewise polynomial function is the best choice. The extracted contours best match the horizon and the visual inspection of the human expert has confirmed this *a priori* supposition.

The texture feature set is composed of two feature subsets: the co-occurrence matrix feature subset and the wavelet decomposition feature subset.

The co-occurrence matrix features are used as structural descriptors and can easily reveal the differences between the three major sediment classes: the sand, the mud, and the rock (see Fig. 13). Other sediment classes may interfere, like the fine sand or other type of rocks. The proposed method can be easily adapted to every horizon shape and is more suitable for small dimension textures.

The use of Wavelet transforms has a large classification score (see Table 2). Its deficiency related to the previous feature subset is the large amount of time

required for processing and the large dimensionality of the resulted features. Therefore, a neural network is used for classification and reduction purposes. This approach is widely used by the scientists who classify sediment-based data [31]. The choice of the mother wavelet is not critical.

The acoustic image database was constructed with responses from different sea campaigns. Their class association was made by the human experts after a visual inspection. As the expert characterization cannot be flawless, the results using the proposed features are not perfect. Although the classification using clustering or neural networks search for hard distinct classes, the human expert characterization is made using a fuzzy logic. Therefore, an appropriate classifier must be considered for future studies.

We estimate that the use of the new feature sets proposed in this article can lead to an automatic sea floor classification system. The approach is novel and currently no automatic alternative exist. Further studies must be carried to integrate the features into a fuzzy classification. Related to the contour, a new feature set can be envisaged, which quantify the fuzziness aspect of the contour.

Acknowledgements: This work was supported by the SHOM Oceanographic Navy Service.

References:

- [1] Jae Adams, E.A. Yfantis, D. Curtis, and Trenton Pack. Feature Extraction Methods for Form Recognition Applications. *WSEAS Transactions on Information Science & Applications*, 3(3):666–671, March 2006.
- [2] Michel Bouvet. *Traitements des signaux pour les systèmes sonar*. Masson, 1992.
- [3] Al Bovik. *Handbook of Image and Video Processing*. Elsevier, 2nd edition, 2005.
- [4] David J. Burdige. *Geochemistry of Marine Sediments*. Princeton University Press, 2006.
- [5] Laurent D. Cohen. On Active Contour Models and Balloons. *Computer Vision, Graphics, and Image Processing*, 53(2):211–218, Mar 1991.

- [6] I. Cojan and M. Renard. *Sédimentologie*. Dunod, 1999.
- [7] T. F. Cootes, C. J. Taylor, D. H. Cooper, and J. Graham. Active Shape Models - Their Training and Application. *Computer Vision and Image Understanding*, 61(1):38–59, Jan 1995.
- [8] R. O. Duda, P. E. Hart, and D. G. Stork. *Pattern Classification*. John Wiley & Sons, Inc., second edition, 2001.
- [9] James D. Foley, Andrie van Dam, Steven K. Feiner, and John F. Hughes. *Computer Graphics. Principles and Practice*. Addison Wesley, 2nd edition, 1997.
- [10] Cedric Gervaise, Nicolas Grangier, and Andre Quinquis. Caracterisation de la lithologie sedimentaire par le coefficient d'attenuation. In *5eme Journees d'Etude d'Acoustique Sous-Marine, Brest, France*, Nov 2000.
- [11] Rafael C. Gonzales and Richard C. Woods. *Digital Image Processing*. Prentice Hall, 3rd edition, 2008.
- [12] Robert M. Haralick. Statistical and Structural Approaches to Texture. *Proceedings of the IEEE*, 67(5):786–804, May 1979.
- [13] Michael Kass, Andrew Witkin, and Demetri Terzopoulos. Snakes: Active Contour Models. *International Journal of Computer Vision*, 1:321–331, 1987.
- [14] Xavier Lurton. *An Introduction to Underwater Acoustics*. Springer, 2002.
- [15] Claire-Sophie Maroni. *Détermination automatique de la stratification des fonds sous-marins à l'aide d'un sondeur de sédiments*. Ph.D. Thesis, Université Bretagne Occidentale, Brest, France, 1997.
- [16] Aleksandra Mojsilović, Miodrag V. Popović, and Dejan M. Rackov. On the Selection of an Optimal Wavelet Basis for Texture Characterization. *IEEE Transactions on Image Processing*, 9(12):2043–2050, Dec 2000.
- [17] Cristian Molder. *Aide à l'interprétation des données sédimentologiques. Analyse de l'information de retrodiffusion entre deux couches par traitement d'images*. M.Sc. Thesis, Université de Brest, Brest, Jun 2001.
- [18] Cristian Molder. Propriétés acoustiques du sous-sol marin mesurées à l'aide d'un sondeur de sédiments. Research report 01/RC/A/11.01, EN-SIETA, Brest, France, 2001.
- [19] Cristian Molder. Propriétés acoustiques du sous-sol marin mesurées à l'aide d'un sondeur de sédiments. Research report 02/RC/A/02.02, EN-SIETA, Brest, France, 2002.
- [20] Cristian Molder. Propriétés acoustiques du sous-sol marin mesurées à l'aide d'un sondeur de sédiments. Research report 03/RC/A/05.02, EN-SIETA, Brest, France, 2002.
- [21] Cristian Molder. Propriétés acoustiques du sous-sol marin mesurées à l'aide d'un sondeur de sédiments. Research report 04/RC/A/10.08, EN-SIETA, Brest, France, 2002.
- [22] Cristian Molder. *Contributions to Pattern Recognition and Classification*. Ph. D. Thesis, Military Technical Academy, Bucharest, Jun 2008.
- [23] Cristian Molder, Helene Thomas, and Andre Quinquis. Texture analysis and marine sediment characterization from acoustical data. In *Proceedings of the 32nd International Scientific Symposium of the Defense Research Agency*, volume 4, pages 237–244, Apr 2001.
- [24] Cristian Molder, Helene Thomas, and Andre Quinquis. Classification des signaux marins par analyse des textures. In *Proceedings of the 13th Reconnaissance de Formes et Intelligence Artificielle Conference (RFIA), Angers, France*, volume 3, pages 799–808, Jan 2002.
- [25] Maria Petrou and Pedro Garcia Sevilla. *Dealing with Texture*. John Wiley & Sons, 2006.
- [26] P. Scheunders, S. Lievens, G. Van de Wouwer, P. Vautrot, and D. Van Dyck. Wavelet-based Texture Analysis. *International Journal Computer Science and Information management*, 1:22–34, 1998.
- [27] Charles H. Sherman and John L. Butler. *Transducers and Arrays for Underwater Sound*. Springer, 2007.
- [28] Mihran Tuceryan and Anil K. Jain. *The Handbook of Pattern Recognition and Computer Vision*, chapter Texture Analysis, pages 207–248. World Scientific Publishing Co., 2nd edition, 1998.

- [29] S. Unterseh. *Cartographie et caractérisation du fond par sondeur multifaisceaux*. Ph.D. Thesis, Institut National Polytechnique de Lorraine, Nancy, France, 1999.
- [30] Constantin-Iulian Vizitiu, Doru Munteanu, and Cristian Molder. A New Version of Flusser Moment Set for Pattern Feature Extraction. *WSEAS Transactions on Information Science & Applications*, 5(4):396–406, April 2008.
- [31] Yu-Ming Wang, Seydou Traore, and Tienfuan Kerh. Monitoring Event-Based Suspended Sediment Concentration by Artificial Neural Network Models. *WSEAS Transactions on Computers*, 7(5):559–568, May 2008.